Journal of Virology

Evidence for pH-Dependent Protease Activity in the Adeno-Associated Virus Capsid

Maxim Salganik, Balasubramanian Venkatakrishnan, Antonette Bennett, Bridget Lins, Joseph Yarbrough, Nicholas Muzyczka, Mavis Agbandje-McKenna and Robert McKenna

J. Virol. **2012, 86(21):11877. DOI: 10.1128/JVI.01717-12. Published Ahead of Print 22 August 2012.**

JVI Journals.ASM.org

Evidence for pH-Dependent Protease Activity in the Adeno-Associated Virus Capsid

Maxim Salganik,[a,b] Balasubramanian Venkatakrishnan,[b,c,d] Antonette Bennett,[b,c,d] Bridget Lins,[b,c,d] Joseph Yarbrough,[b,c,d] Nicholas Muzyczka,[a,b] Mavis Agbandje-McKenna,[b,c,d] and Robert McKenna[b,c,d]

Department of Molecular Genetics and Microbiology,[a] Powell Gene Therapy Center,[b] Department of Biochemistry and Molecular Biology,[c] and Center for Structural Biology,[d] University of Florida College of Medicine, Gainesville, Florida, USA

Incubation of highly purified adeno-associated virus (AAV) capsids *in vitro* at pH 5.5 induced significant autocleavage of capsid proteins at several amino acid positions. No autocleavage was seen at pH 7.5. Examination of other AAV serotypes showed at least two different pH-induced cleavage patterns, suggesting that different serotypes have evolved alternative protease cleavage sites. In contrast, incubation of AAV serotypes with an external protease substrate showed that purified AAV capsid preparations have robust protease activity at neutral pH but not at pH 5.5, opposite to what is seen with capsid protein autocleavage. Several lines of evidence suggested that protease activity is inherent in AAV capsids and is not due to contaminating proteins. Control virus preparations showed no protease activity on external substrates, and filtrates of AAV virus preparations also showed no protease activity contaminating the capsids. Further, N-terminal Edman sequencing identified unique autocleavage sites in AAV1 and AAV9, and mutagenesis of amino acids adjacent to these sites eliminated cleavage. Finally, mutation of an amino acid in AAV2 (E563A) that is in a conserved pH-sensitive structural region eliminated protease activity on an external substrate but did not seem to affect autocleavage. Taken together, our data suggested that AAV capsids have one or more protease active sites that are sensitive to pH induction. Further, it appears that acidic pHs comparable to those seen in late endosomes induce a structural change in the capsid that induces autolytic protease activity. The pH-dependent protease activity may have a role in viral infection.

Adeno-associated virus (AAV) is a nonenveloped single-stranded DNA virus that has a relatively simple capsid consisting of 3 proteins that share a C-terminal amino acid sequence (2). The three capsid proteins (VP1, VP2, and VP3) assemble in an approximate ratio of 1:1:10 to form an icosahedral particle ~246 nm in diameter. Recently the X-ray crystal structure of AAV serotype 8 (AAV8) identified a surface region that undergoes a conformational shift when the virus is incubated at acidic pH (14). This region of four amino acids (the pH quartet) is formed from three different symmetry-related capsids at the intersection of the 2-, 3-, and 5-fold axes. Two of these amino acids, E566 and Y707, interact through hydrogen bonds at pH 7.4 but progressively migrate from each other as the pH is lowered to 6.0 or 5.5, which are the approximate pHs of early and late endosomes. Similar amino acid rearrangements have been seen in the crystal structures of AAV1 (unpublished observation). In AAV2 (Fig. 1), E563 is structurally equivalent to E566 in AAV8, and it is flanked by two other acidic residues (E562 and E564) that are conserved in all AAV serotypes that have been sequenced to date (Table 1). In addition, a tyrosine (Y704), arginine (R389), and histidine (H526) are also highly conserved, as well as another acidic cluster (528DDEE531) near this region (Fig. 1 and Table 1). Acidification of the capsid during virus entry has been shown to be essential for viral infectivity (1, 3, 7), and, thus, the structural shift that occurs in this region may be a key initiation event that is necessary for a critical step in infection. Indeed, we and others previously showed that mutants with mutations in the two conserved acidic domains in AAV2 are up to 6 logs less infectious than wild-type virus even though they assemble normal amounts of mature capsids (10, 13, 22).

Many viruses code for protease activities that are used to process polyproteins during the viral life cycle or to process capsid proteins during viral assembly and capsid maturation (reviewed in reference 8). Recently, Flock House virus (FHV), a nonenveloped insect virus, has been shown to contain a pH-induced protease that is apparently involved in viral trafficking. FHV autocatalytically cleaves a capsid protein to release a peptide that is believed to promote the release of FHV from endosomes (16). The acidic region at the pH quartet site in AAV is reminiscent of acid protease active sites, and this raised the possibility that the AAV capsid may contain a protease activity that is activated in the acidic environment of cellular endosomal compartments. In this article, we test this possibility and show that AAV contains several proteolytic active sites that catalyze autolytic cleavage when the virus is incubated at acidic pH. We also show that the pH quartet region appears to be a pH-sensitive switch that activates a protease or is itself a protease that cleaves external protease substrates.

MATERIALS AND METHODS

Viruses and reagents. AAV1, -2, -5, and -8 virus-like particles (VLPs) were prepared as previously described from baculovirus-infected Sf9 cells for X-ray crystallography (12) and used for the PDQ ("protease determine quick") assay (described below). The recombinant baculoviral vectors

Received 5 July 2012 Accepted 15 August 2012
Published ahead of print 22 August 2012
Address correspondence to Nicholas Muzyczka, muzyczka@mgm.ufl.edu, or Robert McKenna, rmckenna@ufl.edu.
M.S. and B.V. contributed equally to this article.
Supplemental material for this article may be found at http://jvi.asm.org/.

doi:10.1128/JVI.01717-12

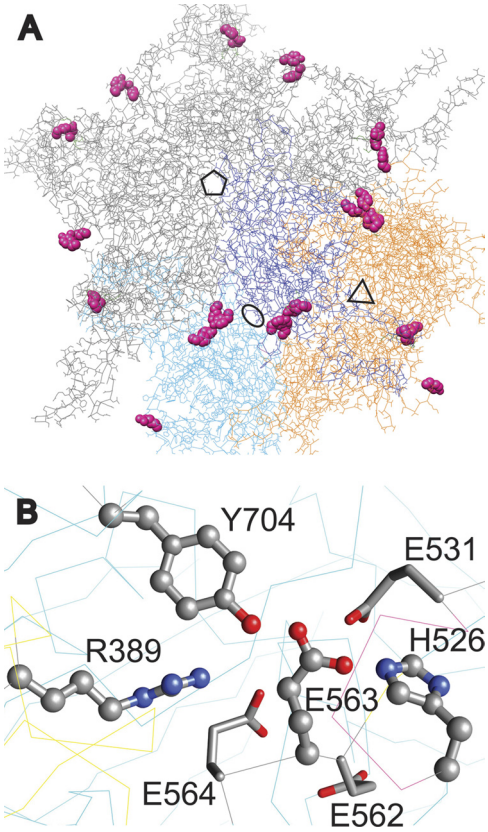

FIG 1 (A) A portion of the AAV2 crystal structure showing a reference capsid protein (blue) that is contained in a pentamer (gray), a trimer (orange), and a dimer (cyan). The pH quartet amino acids are shown in the red space-filling form. The complete cluster is shown flanking the 2-fold axis of symmetry (oval), where all three polypeptide chains contributing to the cluster are present. Smaller clusters are shown at other locations where only one or two of the participating capsid polypeptides are present. The oval, triangle, and pentamer indicate the 2-, 3-, and 5-fold axes of symmetry, respectively. (B) The positions of the pH quartet amino acids in ball-and-stick form (Y704, E563, R389, and H526) in AAV2. These amino acids are potentially interacting through hydrogen bonding. In AAV8, the equivalent amino acids to Y704 and E563 change their positions at acidic pH (14). Also present are two highly conserved glutamates (E562 and E563) and a second charged cluster that contributes E531, all in stick form. Mutations in the two acidic clusters make normal amounts of packaged virus but are extremely defective for infectivity (10, 13, 17, 22).

were a gift from Sergei Zolotukhin (University of Florida). Briefly, for the production of AAV1, -5, and -8, the baculovirus-infected cells were lysed by three freeze-thaw cycles in lysis buffer (50 mM Tris-HCl [pH 8.0], 100 mM NaCl, 1 mM EDTA, 0.2% Triton X-100). Benzonase was added after the second cycle to remove nucleic acid. The samples were cleared by centrifugation at 12,100 × *g* for 15 min at 4°C, and the VLPs were pelleted by sucrose cushion (20% [wt/vol] sucrose in lysis buffer) centrifugation at 149,000 × *g* for 3 h at 4°C. The VLP pellet was further purified by sucrose gradient (10 to 40% [wt/vol] sucrose in 25 mM Tris, 100 mM NaCl, 0.2% Triton X-100, and 2 mM $MgCl_2$) centrifugation at 151,000 × *g* for 3 h at 4°C. For AAV2 VLPs, the cell lysate was purified by centrifugation in a 15-to-60% iodixanol step gradient. The 25% iodixanol fraction, containing VLPs, was further purified by HiTrap Q fast protein liquid chromatography (FPLC) (GE Healthcare) as previously described (23).

AAV1 to -3, AAV5 to -8, and AAV10 virus particles containing a green fluorescent protein (GFP) expression cassette (pTR-UF11) were prepared by DNA transfection in HEK293 cells and purified by iodixanol step gradients and Mono Q FPLC chromatography as previously described (23). AAV9 virus particles (VPs) containing a GFP cassette were purified by iodixanol gradient, washed with 1 M NaCl, and buffer exchanged into 1× phosphate-buffered saline (PBS). In addition, AAV1 containing an α-1-antitrypsin (AAT) cassette (a kind gift from David Knop at Applied Genetic Technologies Corporation [AGTC], Gainesville, FL) was made by an alternative protocol using herpesvirus-infected BHK cells and purified as previously described (19). Briefly, BHK cells growing in suspension were coinfected with two recombinant herpes simplex virus (rHSV) vectors and then simultaneously lysed and digested (1% [vol/vol] Triton X-100, 25 U/ml Benzonase, 2 mM $MgCl_2$) 24 h later. The lysate was filter clarified and then column purified by CIM Q (BIA Separations) and affinity (AVB; GE Healthcare) chromatography. The GFP-containing virus particles were used for autoproteolysis assays as described below. AAV1 containing an AAT cassette was used for AAV1 mass spectroscopy and Edman sequencing. Virus stocks for autoproteolysis made by DNA transfection were obtained from the University of Florida Vector Core Laboratory (AAV1, -2, -5, -8, and -9), Sergei Zolotukhin (rh10), Mavis Agbandje-McKenna (AAV3 and -6), and Roland Herzog (AAV7).

Mouse monoclonal antibodies A1 and B1 were a kind gift from Jurgen Kleinschmidt (21). A1 recognizes an epitope unique to VP1 (amino acids [aa] 123 to 131) in both AAV1 and AAV2. B1 recognizes an epitope present in all three capsid proteins (aa 725 to 735) that is conserved in all serotypes except AAV4.

The Halt protease inhibitor single-use cocktail was obtained from Thermo Scientific and used according to the manufacturer's instructions. The PDQ protease assay kit (Athena enzyme systems) was used as recommended by the manufacturer. The PDQ assay is a colorimetric assay used to detect protease activity in aqueous samples. The PDQ proprietary substrate is a casein derivative entrapped in a cross-linked matrix with a dye conjugate that responds to a wide range of proteases, including serine protease, metalloprotease, and aspartate and cysteine proteases.

Protease assays. The protease activities of the AAV1, -2, -5, and -8 VLPs and GFP-containing AAV8 were determined using the PDQ protease assay kit. Each assay contained 500 μl of virus sample (0.1 mg/ml, 30 nM virus particles) or 30 nM serine protease trypsin as a positive control. Negative controls included carbonic anhydrase (also at 30 nM [data not shown]), buffer with no enzyme, or a mock VLP preparation purified from mock-infected cells in the same way as viral VLPs. A portion of the AAV8 GFP preparation was further purified by passage through an Amicon 100-kDa-molecular-mass-cutoff filter, and both the filtrate and the virus fraction were assayed for protease activity to ensure that the protease activity was not a result of a contaminating cellular protease in the virus sample. Each sample was loaded into the assay vial containing the PDQ proteolytic substrate, at pH 7.5 (20 mM Tris-HCl) or pH 5.5 (20 mM citrate buffer), with or without protease inhibitors (10 μl/ml [vol/vol]). The time course of protease activity was monitored with samples collected hourly

TABLE 1 Alignment of amino acid residues that contribute to the pH quartet in AAV1 to -10

AAV	Residue(s) at position(s)[a]: 389	526	528–531	561–564	704
AAV1	**R**	H	DDED	DEEE	Y
AAV2	**R**	H	DDEE	DEEE	Y
AAV3	**R**	H	DDEE	DEEE	Y
AAV4	**R**	A	PADS	SEEE	Y
AAV5	**R**	N	LQGS	SESE	Y
AAV6	**R**	H	DDKD	DEEE	Y
AAV7	**R**	H	DDED	NEEE	F
AAV8	**R**	H	DDEE	SEEE	Y
AAV9	**R**	H	EGED	NEEE	Y
AAV10	**R**	H	DDEE	SEEE	Y

[a] The numbering is according to AAV2. Boldface residues are identical in all known serotypes sequenced to date.

for a total of 5 h. The reaction was arrested by adding 500 μl of 0.2 N NaOH, the samples were centrifuged, and absorbance was measured in a Beckmann spectrophotometer at 450 nm. Each assay was repeated three times, and the data were analyzed with Graph Pad Prism 5 statistical software using repeated-measures two-way analysis of variance (ANOVA) with Bonferroni's post-test.

Autoproteolysis assay. Viruses containing a GFP expression cassette, which were made by the DNA transfection method, were used for autoproteolysis, mass spectroscopy (MS), and Edman sequencing. Approximately 1×10^{10} viral genome-containing particles were incubated in either 1× PBS (pH 7.4) or 0.1 M citrate buffer (pH 5.5) for 1 h at 37°C. Samples were incubated at 95°C for 5 min in the presence of Laemmli buffer, separated by SDS-PAGE using 4 to 20% gradient gels, and transferred onto Immun-Blot polyvinylidene difluoride (PVDF) membranes (0.2-μm pore size; Bio-Rad, Hercules, CA). Membranes were blocked (5% milk) and probed with either B1 (1:3,000) or A1 (1:20) monoclonal antibody for 1 h at room temperature, followed by incubation with anti-mouse horseradish peroxidase (HRP)-conjugated (1:5,000) secondary antibodies (GE Healthcare Bioscience, Pittsburgh, PA) and enhanced chemiluminescence (ECL) visualization. Estimation of fragment sizes was done with ImageQuant TL software (GE Healthcare Bioscience, Pittsburgh, PA) analysis of scanned immunoblots using Precision Plus prestained protein size standards (Bio-Rad, Hercules, CA).

MS and Edman sequencing. Mass spectroscopy (MS) analysis was conducted on AAV1-AAT cleavage fragments with sizes of ~17 kDa and ~50 kDa. Prior to analysis, 1×10^{11} genome-containing particles were subjected to autoproteolysis at acidic pH as described above. Fragments were then separated by SDS-PAGE as described above, and cleavage bands were visualized by staining the gel with biosafe Coomassie blue (Bio-Rad; Hercules, CA). The desired cleavage bands were excised with a scalpel and submitted to the Protein Core of the University of Florida Interdisciplinary Center for Biotechnology Research, where they were treated with 100 mM iodoacetamide (45 min at room temperature) and trypsin in preparation for MS analysis. Peptides were extracted from the gel slices with 200 μl 80:20 acetonitrile-water containing 0.1% formic acid and vacuumed to dryness. Samples were dissolved in 3% acentonitrile, 0.1% acetic acid, and 0.01% trifluoroacetic acid (TFA). Liquid chromatography-tandem MS (LC-MS/MS) analysis was carried out on a LTQ Orbitrap XL mass spectrometer (ThermoFisher Scientific, West Palm Beach, FL). All MS/MS samples were analyzed with Mascot version 2.2.2 (Matrix Science, London, United Kingdom). Scaffold version 3.0.9.1 (Proteome Software, Inc., Portland, OR) was used to validate MS/MS-based peptide and protein identifications. Peptide identifications were accepted if they could be established at greater than 95.0% probability, as specified by the Peptide Prophet algorithm (9). Protein identifications were accepted if they could be established at greater than 99.0% probability and contain at least 2 identified unique peptides. Protein probabilities were assigned by the Protein Prophet algorithm (15).

For Edman sequencing, 2×10^{12} genome-containing AAV1-AAT or AAV9-GFP particles were subjected to acidic autoproteolysis. The samples were then boiled in Laemmli buffer and concentrated to 30 μl by vacuum centrifugation. The concentrated samples were buffer exchanged into 10 mM Tris-HCl using Micro Bio-spin 6 size exclusion columns per the manufacturer's instructions (Bio-Rad, Hercules, CA). Samples were then separated by gradient SDS-PAGE as previously described and transferred to Immobilon P^{SQ} PVDF membranes (Millipore, Billerica, MA). Membranes were washed with double-distilled H_2O (ddH_2O) and then stained with fresh Coomassie R-250 brilliant blue for 30 s followed by destaining with 40% methanol–5% acetic acid. Membranes were washed 3 times with ddH_2O and allowed to air dry prior to cutting of bands. Individual bands were submitted for N-terminal sequencing (Edman degradation) to Alphalyse (Palo Alto, CA).

AAV1, -2, and -9 capsid mutants. Mutants were constructed using the Quikchange II site-directed mutagenesis kit (Agilent Technologies; Santa Clara, CA). Mutants were made in either a pXR1 (AAV1), pRep2Cap9 (AAV9), or pIM45 (AAV2) background. The mutants were confirmed by sequencing through the entire cap open reading frame (ORF). Mutant viruses were prepared by polyethylenimine transfection of 5- by 15-cm^2 plates of HEK293 cells and purified by iodixanol step gradient centrifugation as previously described (23). All mutant viruses were packaged with pTR-UF11 containing a GFP expression cassette. After iodixanol centrifugation, the material from the 40%/60% interface was washed in a 150-kDa-cutoff concentrator (Apollo; Orbital Bioscience, Topsfield, MA) with 50 ml of 1× TD (1× PBS plus 1 mM $MgCl_2$ and 2.5 mM KCl) plus 1 M NaCl. The virus was then buffer exchanged into 1× PBS (pH 7.4) and concentrated to 500 μl. Titer determination was done by real-time PCR using SYBR green supermix and the MyIQ thermal cycler (Bio-Rad, Hercules, CA) with primers against the chicken β-actin (CBA) promoter: forward (FWD), TCCCATAGTAACGCCAATAGG; and reverse (REV), CATCAAGTGTATCATATGCCAAG. Equal amounts of genome-containing particles were then used to compare the mutants to the wild type in the autoproteolysis assay.

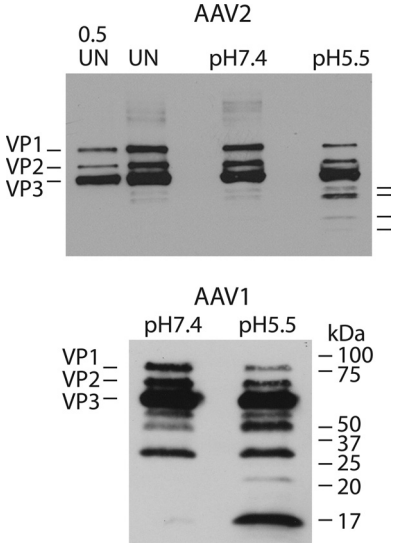

FIG 2 AAV undergoes autolytic cleavage at pH 5.5. (Top) Approximately 100 fmol (10^{10} particles) of AAV2 was either untreated (UN) or incubated at pH 7.4 or pH 5.5 for 60 min at 37°C and then electrophoresed on an SDS-acrylamide gel and immunoblotted with B1 antibody, which recognizes a common epitope present at the C-terminal end of all three capsid proteins. The "0.5 UN" lane contains half the amount of virus shown in the UN lane and allows estimation of the loss of VP1 and 2 in the pH 5.5 lane. The positions of the VP1, -2, and -3 bands and several cleavage bands are also indicated to the left and right, respectively. (Bottom) AAV1 was treated at pH 7.4 or pH 5.5 for 60 min at 37°C, electrophoresed on an SDS-acrylamide gel, and immunoblotted with B1 antibody.

RESULTS

AAV undergoes autolytic proteolysis at low pH. To see if AAV undergoes pH-induced protease cleavage, a purified preparation of AAV2 was incubated for 60 min at pH 7.4 or pH 5.5, and the molecular mass of the three capsid proteins was examined by immunoblotting with B1 antibody, a capsid antibody that recognizes an epitope near the C-terminal end of the capsid protein (21). Virus that was treated at pH 7.4 showed no change in the integrity of the three capsid proteins compared to untreated virus (Fig. 2; AAV2). However, virus that was treated at pH 5.5 showed a decrease of the two larger capsid proteins, VP1 and VP2, as well as the appearance of several new lower-molecular-mass viral bands or an increase in their intensity. Treatment of AAV1 at low pH

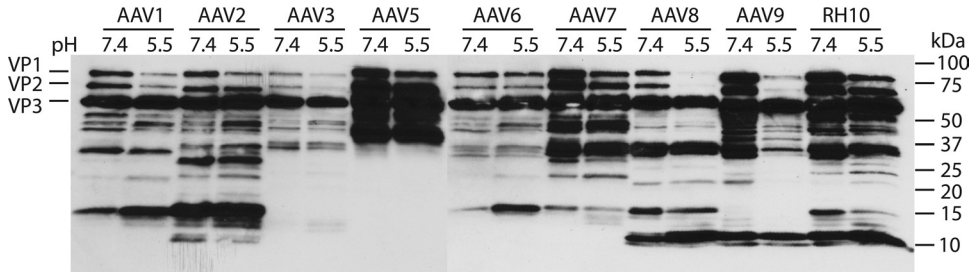

FIG 3 All of the AAV serotypes undergo autolytic cleavage. Serotypes 1 to 3 and 5 to 10 were incubated at pH 7.4 and 5.5 as described in the legend to Fig. 2 and immunoblotted with B1 antibody.

produced similar changes in the B1 immunoblot pattern (Fig. 2; AAV1), namely, a decrease in VP1 and -2 and an increase in several lower-molecular-mass bands.

Two of the cleavage bands that were produced when AAV1 was incubated at pH 5.5, ~17 kDa and ~55 kDa, were isolated by gel electrophoresis and subjected to MS analysis to identify the approximate positions of the cleavage sites (see Fig. S1 in the supplemental material). The 17-kDa band generated peptides that clustered near the C terminus of the capsid protein, as expected, but also generated peptides located in the middle of the capsid and at the N terminus. The same was seen with the 55-kDa band. This suggested that both the 17-kDa and 55-kDa bands contained multiple capsid cleavage products, and this was consistent with at least two and probably more proteolytic cleavage sites in the capsid.

To check for the possibility that a cellular protease might be contaminating the virus preparations, the untreated AAV1 preparations were also analyzed by MS. No proteins other than the three AAV capsid proteins were consistently found in the virus stocks. Trypsin, which had been added to cleave the capsid proteins during mass spectroscopy, was the only protease found, but previous mapping of the trypsin sites on AAV capsids (20) was not consistent with the cleavage patterns seen following pH 5.5 autocleavage.

The effect of pH 5.5 on the other AAV serotypes was similar (Fig. 3). In all cases, there was a significant decrease of VP1 and VP2 and the appearance of additional lower-molecular-mass bands (or an increase in their intensity) when the viruses were incubated at pH 5.5. Comparison of the cleavage patterns seen in the different serotypes suggested that there were several different cleavage patterns as well as multiple cleavage sites in each serotype. For example, AAV1, -2, and -3 produced an approximately 17-kDa C-terminal peptide, while AAV8, -9, and -10 produced an ~10-kDa C-terminal band. Taken together, it appeared that all AAV serotypes were capable of some autolytic activity and that this activity was activated by low pH.

AAV can cleave an external protease substrate. To see if AAVs can also cleave an external substrate, the PDQ colorimetric protease assay was used (see Materials and Methods). Incubation of AAV1, -2, -5, and -8 at a 30 nM capsid concentration with the protease substrate showed robust protease activity for each. The protease activity in the capsids was comparable (within 2-fold) to that seen with 30 nM trypsin (Fig. 4A). However, unlike autolytic cleavage, which was activated by low pH, cleavage of the external substrate was only observed at pH 7.5 and was largely abolished at pH 5.5. In addition, cleavage of the PDQ substrate by all serotypes was abolished by the addition of protease inhibitors (Fig. 4C).

The possibility that the capsids might be contaminated by a cellular protease that copurified with capsid was also tested. Control cell extracts that had been purified the same way as capsid preparations were negative for protease activity (Fig. 4B; mock infected). In addition, a portion of the AAV8 stock was filtered through a concentrator (Amicon) that would retain the 3×10^6-kDa capsid but permit a 100-kDa soluble protease to flow through. When both the material that passed through the filter and the capsids were tested for protease activity, the capsid fraction retained all of the protease activity (Fig. 4D).

A capsid mutation in the pH quartet completely eliminates protease activity on external substrates but not autolytic cleavage. To see if E563, which had been identified as a pH-sensitive amino acid by X-ray crystallography in AAV8, was essential for external protease activity, it was mutated to an alanine in AAV2. The E563A mutation completely abolished protease activity on an external substrate (Fig. 4B). However, when we tested the ability of this mutant to carry out autolytic cleavage of the capsid, there appeared to be no change in its ability to cleave capsid proteins (Fig. 5). In addition, mutants with mutations in amino acids that flanked the E563 position and were completely conserved in all AAV serotypes, E562A and E564A, also appeared to be capable of autolytic cleavage. A fourth mutant, E561A, as well as a previously isolated mutant (22) that contained all four of these acidic residues mutated to alanine (Mut40; E561 to 564A), also shared this phenotype (Fig. 5). Taken together, these findings suggested a possible model in which the pH quartet region might not itself be a protease active site but instead might be acting like a pH-sensitive switch that induces a structural change in the capsid. This in turn activates protease sites throughout the capsid or represses them.

Identification of specific cleavage sites induced at pH 5.5. To identify specific autolytic cleavage sites, two serotypes were chosen for Edman sequencing, AAV1 and -9. These serotypes were chosen because both were available in large quantity and produced pH-induced cleavage fragments that could be separated from contaminating fragments. Table 2 shows that the apparent 10-kDa band produced by AAV9 was the result of cleavage between amino acids (aa) 657 and 658 and has a calculated molecular mass of 9.3 kDa. Similarly, the apparent 17-kDa band from AAV1 came from a cleavage between aa 590 and 591 to produce a fragment that has a calculated molecular mass of 16.3 kDa. Finally, a 40-kDa band from AAV1 was cleaved between aa 219 and 220. Its molecular mass was apparently the result of cleavage at both the 219 and 590 positions, thus producing the apparent 40-kDa band isolated from the gel.

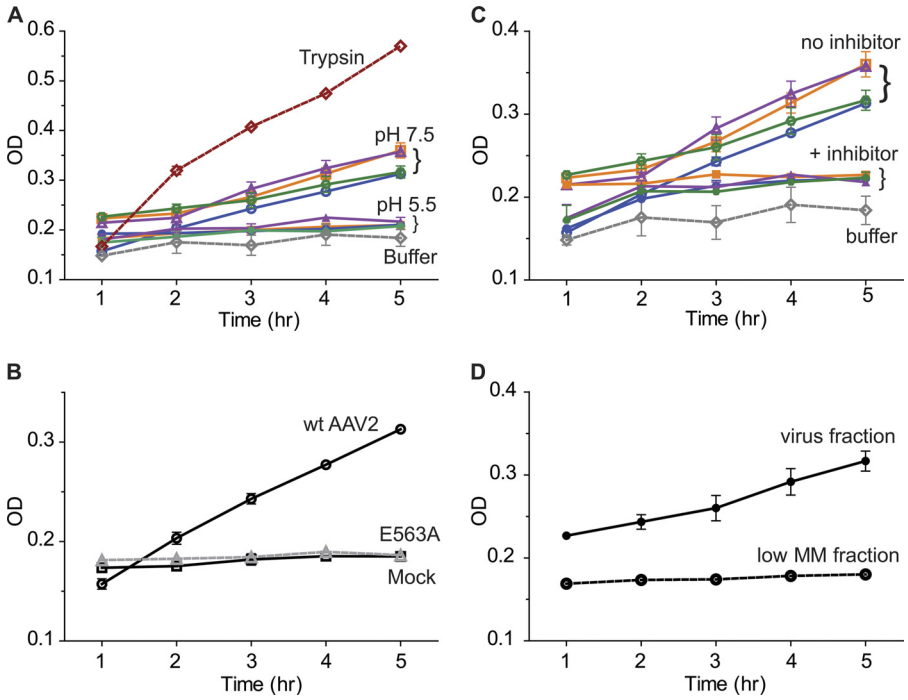

FIG 4 The AAV capsid can cleave an external protein substrate. (A) The PDQ colorimetric protease assay was used to compare the protease activity of AAV serotypes at pH 7.5 (open symbols) and pH 5.5 (closed symbols) to those of trypsin at pH 7.5 (red diamonds) and the no-enzyme control (buffer; gray diamonds). AAV1, orange squares; AAV2, blue circles; AAV5, purple triangles; AAV8, green hexagons. (B) The E563A mutant abolishes protease activity. The protease activities of wild-type (wt) AAV2 VLPs (circles) were compared to those of the E563A mutant (squares) and to a mock virus extract (gray triangles with dotted line). (C) Virus was incubated at pH 7.4 with PDQ protease substrate for 1 to 5 h in the presence (closed symbols) or absence (open symbols) of protease inhibitor (Halt protease inhibitor cocktail; see Materials and Methods) and compared to the no-enzyme control (gray diamonds with dotted line). AAV1, orange squares; AAV2, blue circles; AAV5, purple triangles; AAV8, green hexagons. (D) AAV8 was fractionated through a 100-kDa filter (Amicon), and the flowthrough (low molecular mass [MM]) fraction and retained (virus) fractions were tested for protease activity.

Identification of putative active site amino acids. The position 657 cleavage site in AAV9 is part of the so-called HI loop, a loop that surrounds the 5-fold pore and extends from one asymmetric unit over a neighboring unit in the pentamer (Fig. 6A). The site is surrounded by several amino acids that could participate in acid-induced cleavage, including D657, S669, Y674, and T676 (Fig. 6B). Each of these amino acids was individually mutated to alanine and tested for its ability to cleave at position 657 to produce the diagnostic 10-kDa C-terminal fragment. Mutation of D657 completely abolished production of the 10-kDa fragment (Fig. 6C). Mutation of S669 and T676 did not affect cleavage at 657; however, these mutants appeared to be unable to produce a fragment of approximately 30 kDa that was present in wild-type AAV9. Finally, mutation of amino acid 674 produced capsid proteins that could no longer assemble, consistent with its location at a 5-fold interface. Such viruses typically degrade their monomer capsid protein, and, thus, no capsid protein was detected. The ability of D657A to transduce HEK293 cells when the virus con-

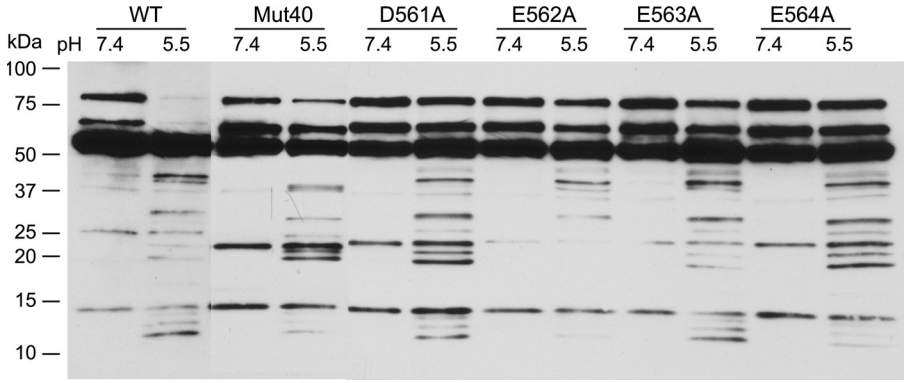

FIG 5 The E563A mutation and mutations in flanking acidic amino acids do not abolish autolytic cleavage of AAV2. Wild-type (WT) and mutant virus preparations were incubated at pH 7.4 and 5.5 as described in the legend to Fig. 2 and immunoblotted with B1 antibody. Mut40 contains all four of the other acidic mutations.

TABLE 2 Edman N-terminal sequences

AAV	Cleavage site	Confidence (%)	Cleavage sequence[a]	Mol mass (kDa) of: C-terminal fragment	Mol mass (kDa) of: Gel fragment
AAV1	590	100	TD/PATGDV	16.3	17
	219	90	AD/GVGNAs	58.1	40
AAV9	657	90	AD/PPTAFN	9.3	13

[a] Lowercase indicates a mismatch with the published sequence, and underlining indicates that more than one amino acid was detected at the position.

tained a GFP expression cassette was also tested. Although AAV9 does not efficiently infect cells in culture, no major difference between D657A and wild-type virus transduction efficiencies was detected when equal amounts of wild-type virus and mutant virus were compared (data not shown).

A similar set of experiments was carried out to identify amino acids involved in the AAV1 cleavage at position 590, which is located on the capsid surface at the top of the three protrusions surrounding the icosahedral 3-fold axes (Fig. 7A). Four amino acids in the vicinity of position 590 (aa 590, 593, 504, and 583) were changed to alanine residues (Fig. 7B). Of these, only the E590A mutation eliminated cleavage at the 590 position when the products of the cleavage reaction were immunoblotted with B1 antibody (Fig. 7C).

The VP1 cleavage pattern is different from that of VP3. The cleavage products from wild-type AAV1 were also immunoblotted with A1 antibody. This monoclonal antibody recognizes an epitope that is present only at the N terminus of VP1 (21) and would visualize only VP1-related cleavage products. When this was done, approximately 60% of AAV1 VP1 was cleaved in 30 min, and three new A1-positive bands were produced or increased in intensity (Fig. 8). Thus, in AAV1, there were a minimum of three pH-induced cleavage sites within VP1.

The prominent band at ~67 kDa was expected and is consistent with cleavage at aa 590 (Table 1). (Note that full-length VP1 is 81.4 kDa, so 81.4 − 16.3 kDa = 65.1 kDa.) However, a band at 23 kDa was also expected due to cleavage at aa 219, and this band was not detected from VP1 (Fig. 8). Thus, cleavage at position 219 occurs only in VP3, and possibly VP2, but not in VP1.

Finally, it should be noted that one of the bands present at pH 7.4 was not significantly increased in intensity at pH 5.5 (Fig. 8; ~50 kDa). This band, therefore, may be due to cleavage by a cellular protein, either during capsid assembly or during virus purification. Bands that did not respond to pH induction were also seen in B1 antibody immunoblots (Fig. 2 and 3).

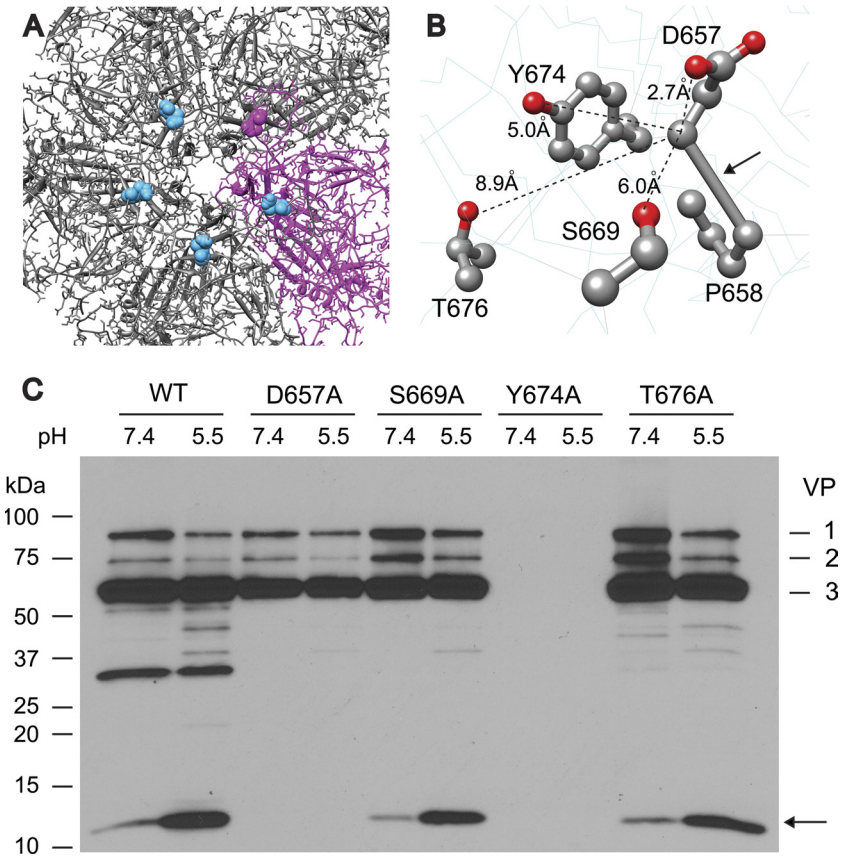

FIG 6 (A) AAV9 amino acids 657 and 658 (blue and red space-filling molecules) are illustrated on the AAV9 pentamer (gray and red). The reference molecule (red subunit) illustrates that the cleavage site is located on the HI loop, which extends over the nearest neighbor capsid protein in the pentamer. (B) The amino acids near the site of the 657/658 peptide bond (arrow) that were potentially involved in the position 657 cleavage reaction were substituted for with alanine residues and tested for autolytic cleavage activity at position 657. (C) Wild-type (WT) AAV9 and mutant AAV9 were incubated at pH 7.4 or 5.5 at 37°C for 60 min and immunoblotted with B1 antibody.

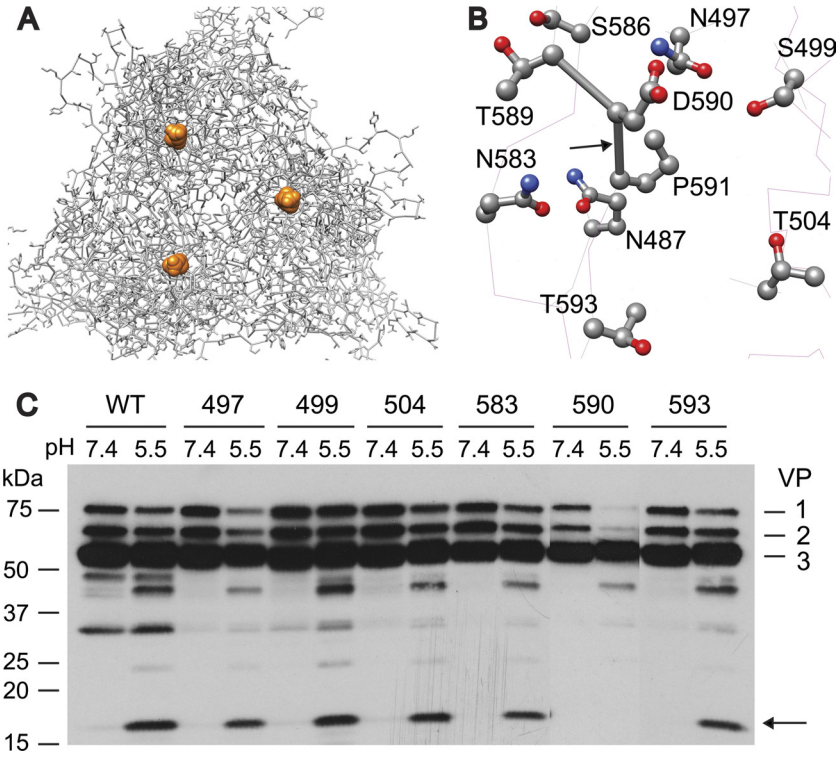

FIG 7 (A) AAV1 amino acids 590 and 591 (gold space-filling molecules) are illustrated on the AAV1 trimer (gray). (B) The amino acids near the site of the 590-591 peptide bond (arrow) that were potentially involved in the position 590 cleavage were substituted with alanine residues and tested for autolytic cleavage activity at position 590. (C) Wild-type (WT) AAV1 and mutant AAV1 were incubated at pH 7.4 or 5.5 at 37°C for 60 min and immunoblotted with B1 antibody.

DISCUSSION

AAV particles have an intrinsic protease activity. We have presented evidence that the AAV capsid contains protease activity. Several lines of evidence support this conclusion. First, we showed that purified VLPs of serotypes 1, 2, 5, and 8 were capable of cleaving an external protease substrate, and the activity was sensitive to protease inhibitors. Furthermore, a single substitution mutation in AAV2, E563A, completely abolished AAV2 protease activity on an external substrate. In addition, size fractionation of the AAV8 preparation to remove any potential low-molecular-mass protease contaminants (<100 kDa) showed that protease activity copurified with the AAV capsid.

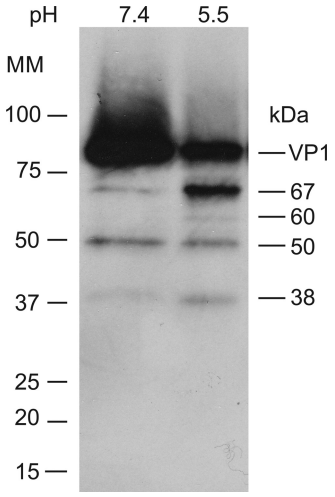

FIG 8 AAV1 was incubated at pH 7.4 or 5.5 for 60 min at 37°C as described in the legend to Fig. 2 and then immunoblotted with A1 antibody, which recognizes an epitope that is present only in VP1. MM, molecular mass.

We also demonstrated that all of the AAV serotypes tested (AAV1 to -3 and AAV5 to -10) were capable of autolytic cleavage at multiple sites within the capsid. This activity was induced by incubation at pH 5.5, the approximate pH of late endosomes. When we mapped two of the cleavage sites in AAV1 (Fig. 9), one of them was at amino acid (aa) 219, a position that is located in the interior of the AAV1 capsid (unpublished observation). Since it was unlikely that a contaminating cellular protease could enter the capsid through the 5-fold pore, cleavage at aa 219 is likely to be autocatalytic. In addition, MS analysis of the AAV1 preparation failed to reveal a contaminating protease other than the one added to perform MS. It is also worth noting that the virus preparations used in this study were isolated using three different production and purification methods (baculovirus infection, herpesvirus infection, and DNA transfection) and contained both full and empty capsids. Finally, as in most autocleavage reactions, one of the amino acids at the site of cleavage was essential for autolytic cleavage. Mutation of both AAV9 D657 and AAV1 D590 to alanine abolished cleavage at these positions. Taken together, our evidence supports the conclusion that the AAV capsid has intrinsic protease activity.

The pH quartet may be a pH switch that controls protease activity. A curious aspect of our data was that protease activity on an external substrate and autolytic protease activity had different pH sensitivities. Autolytic protease activity was induced by pH 5.5

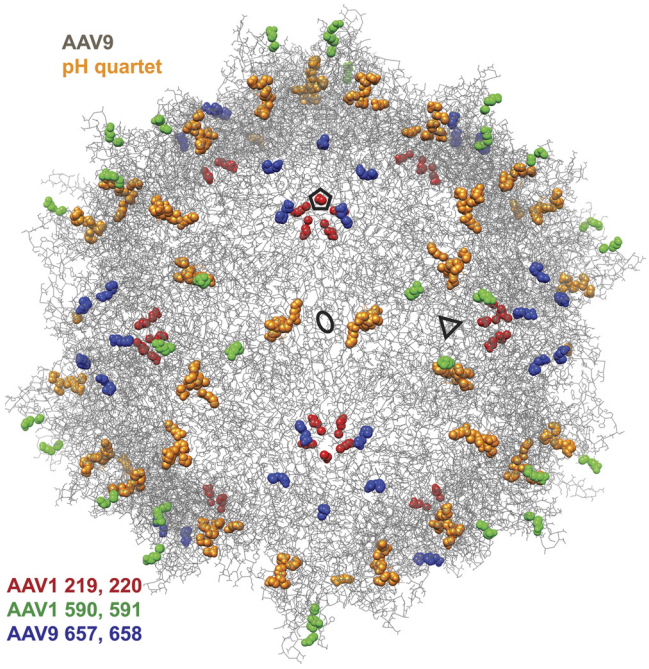

FIG 9 The position of the pH quartet region (orange) is shown in space-filling models on the gray wire background of the AAV9 crystal structure. The AAV9 position 657 cleavage site (blue), the AAV1 219 site (red), and the AAV1 590 (green) cleavage site are also shown as space-filling models. The oval, pentamer, and triangle indicate the positions of the 2-, 5-, and 3-fold axes, respectively.

and was not active at pH 7.4. In contrast, protease activity on an external substrate was seen only at pH 7.5, not at pH 5.5. Moreover, external protease activity was completely eliminated by the E563A mutation in AAV2, an amino acid structurally equivalent to one that had previously been seen to undergo a structural change when AAV8 crystals were examined at pH 5.5 (14). In contrast, autolytic cleavage appeared not to be affected by this mutation. Autolytic cleavage was eliminated only by mutation of acidic residues at the sites of cleavage (amino acids 590 and 657). In addition, we note that some of the autolytic cleavage sites were already cleaved in some viral samples that had been prepared and purified at neutral pH. We interpret this to mean that cleavages can occur at neutral pH at a reduced rate and accumulate over time.

The positions of these pH-sensitive sites are illustrated in Fig. 9. It is immediately apparent that all of the cleavages that were mapped (amino acids 219, 590, and 657) are well separated from the pH quartet region. Both D657 and D219 are near the 5-fold pore, outside and inside the capsid, respectively, while D590 is located at the protrusions surrounding the 3-fold axis. This begs the question is there one protease active site that participates in all of these cleavages or multiple active sites? Typically, acid protease active sites have two acidic amino acids that coordinate a water molecule that is the nucleophile. An intriguing possibility is that the N-terminal sequences of VP1 or VP2, which are the only regions in the capsid that are not structurally constrained, may supply the second acidic residue that participates at multiple sites. In this regard, we note that when we examined the cleavage of VP1 using an antibody specific for this capsid protein, we did not see cleavage at residue 219. This would have produced a 23-kDa N-terminal fragment from VP1; thus, cleavage at 219 apparently occurs only in VP3, and perhaps VP2.

As mentioned earlier, the pH quartet region contains amino acids from three symmetry-related VP3s that are near the intersection of the 2-, 3-, and 5-fold axes (Fig. 9). It was identified as one of two sites in the AAV8 capsid that undergoes an ordered structural shift when viral crystals are incubated at pH 5.5 (14). Mutations in the equivalent region of AAV2 are capable of assembly and DNA packaging but have significant defects in their ability to transduce cells (10, 13, 17, 22). The nature of the defect has not been identified but appears to occur at a postentry step, in viral trafficking, uncoating, or gene expression (unpublished observation). It has also been shown by several groups that exposure to the acidic environment of cellular endosomes is an essential step for viral infection (1, 3, 7). Taken together, these facts suggest that the pH quartet region and the induction of protease activity perform an essential function in the viral life cycle.

One consequence of passage through the acidic endosomal compartment is the extrusion of the N terminus of VP1, which contains both nuclear localization sites and a phospholipase activity that are essential for infection (5, 6, 11). Although treatment of virus with acidic pH *in vitro* does not in itself induce exposure of the VP1 N terminus, passage through acidic endosomes appears to be essential (18). Thus, acidification (plus some other process that occurs during entry and has not yet been identified) is essential for VP1 extrusion and infectivity. We note that the autonomous parvovirus minute virus of mice (MVM) undergoes cleavage of its major capsid protein VP2 approximately 22 amino acids from its N terminus, either sometime after assembly or during cell entry. This cleavage is believed to be due to one or more cellular proteases and is important for the subsequent extrusion of the VP1 N terminus (4). It is therefore tempting to speculate that the pH quartet region is a pH-sensitive "molecular switch" that induces a structural change in the capsid, thereby exposing protease active sites within the capsid at several locations (Fig. 9; amino acids 219, 590, and 657). This in turn may facilitate extrusion of VP1 to the capsid surface. The identification of cleavage sites both external to the 5-fold pore and immediately internal to the pore (Table 2 and Fig. 9; amino acids 657 and 219) supports the possibility that the role of capsid cleavage may be to prepare the capsid for VP1 extrusion. Alternatively, cleavage of the capsid at several locations may be essential to promote viral uncoating once the virus enters the nucleus. However, mutation of E563, at least in the context of the AAV2 serotype, did not noticeably change the pH induction of autolytic protease activity (Fig. 5). Thus, if the pH quartet is indeed a molecular switch, additional cofactors provided by the cell may be required.

An alternative model is that the pH quartet is itself a protease that is active only on an external substrate and the other cleavages that we have mapped (amino acids 219, 590, and 657) are independent pH-sensitive active sites. This possibility suggests that the role of the pH quartet region, which includes E563, is to cleave only an external substrate during entry (i.e., some cellular protein that must be cleaved for efficient infection). However, this model would then suggest that AAV particles contain multiple protease active sites that are independently controlled by pH. We are not aware of a precedent for this in other viruses.

In conclusion, we believe we have evidence for a viral protease within the AAV capsid, but as yet, we do not fully understand its mechanism or its purpose.

ACKNOWLEDGMENTS

We thank David Knop of AGTC, Inc., for providing highly purified AAV1 containing an AAT cassette. We thank Sergei Zolotukhin and Roland Herzog for AAV rh10 and AAV7, respectively.

This work was supported by NIH grants to R.M., M.A.M, and N.M. (HL59412, HL51811, GM082946, and AI081961). N.M. was also supported by the Edward R. Koger American Cancer Society Endowment Fund. M.S. and B.V. were supported by University of Florida Alumni and Grinter Fellowships. J.Y. was supported by the HHMI Science for Life program.

N.M. is an inventor of patents related to rAAV technology and owns equity in a gene therapy company that is commercializing AAV for gene therapy applications.

REFERENCES

1. **Bartlett JS, Wilcher R, Samulski RJ.** 2000. Infectious entry pathway of adeno-associated virus and adeno-associated virus vectors. J. Virol. **74**: 2777–2785.
2. **Berns KI, Parrish CR.** 2007. Parvoviridae, p 2437–2477. *In* Knipe DM, Howley PM (ed), Fields virology, 5th ed. Lippincott Williams and Wilkins, New York, NY.
3. **Douar AM, Poulard K, Stockholm D, Danos O.** 2001. Intracellular trafficking of adeno-associated virus vectors: routing to the late endosomal compartment and proteasome degradation. J. Virol. **75**:1824–1833.
4. **Farr GA, Cotmore SF, Tattersall P.** 2006. VP2 cleavage and the leucine ring at the base of the fivefold cylinder control pH-dependent externalization of both the VP1 N terminus and the genome of minute virus of mice. J. Virol. **80**:161–171.
5. **Girod A, et al.** 2002. The VP1 capsid protein of adeno-associated virus type 2 is carrying a phospholipase A2 domain required for virus infectivity. J. Gen. Virol. **83**:973–978.
6. **Grieger JC, Johnson JS, Gurda-Whitaker B, Agbandje-McKenna M, Samulski RJ.** 2007. Surface-exposed adeno-associated virus Vp1-NLS capsid fusion protein rescues infectivity of noninfectious wild-type Vp2/Vp3 and Vp3-only capsids but not that of fivefold pore mutant virions. J. Virol. **81**:7833–7843.
7. **Hansen J, Qing K, Srivastava A.** 2001. Adeno-associated virus type 2-mediated gene transfer: altered endocytic processing enhances transduction efficiency in murine fibroblasts. J. Virol. **75**:4080–4090.
8. **Johnson JE, Vogt PK.** 2010. Cell entry by non-enveloped viruses. Curr. Top. Microbiol. Immunol. 343:v–vii.
9. **Keller A, Nesvizhskii AI, Kolker E, Aebersold R.** 2002. Empirical statistical model to estimate the accuracy of peptide identifications made by MS/MS and database search. Anal. Chem. **74**:5383–5392.
10. **Kern A, et al.** 2003. Identification of a heparin-binding motif on adeno-associated virus type 2 capsids. J. Virol. **77**:11072–11081.
11. **Kronenberg S, Bottcher B, von der Lieth CW, Bleker S, Kleinschmidt JA.** 2005. A conformational change in the adeno-associated virus type 2 capsid leads to the exposure of hidden VP1 N termini. J. Virol. **79**:5296–5303.
12. **Lane MD, et al.** 2005. Production, purification, crystallization and preliminary X-ray analysis of adeno-associated virus serotype 8. Acta Crystallogr. Sect. F Struct. Biol. Cryst. Commun. **61**:558–561.
13. **Lochrie MA, et al.** 2006. Mutations on the external surfaces of adeno-associated virus type 2 capsids that affect transduction and neutralization. J. Virol. **80**:821–834.
14. **Nam HJ, et al.** 2011. Structural studies of adeno-associated virus serotype 8 capsid transitions associated with endosomal trafficking. J. Virol. **85**: 11791–11799.
15. **Nesvizhskii AI, Keller A, Kolker E, Aebersold R.** 2003. A statistical model for identifying proteins by tandem mass spectrometry. Anal. Chem. **75**: 4646–4658.
16. **Odegard AL, et al.** 2009. Low endocytic pH and capsid protein autocleavage are critical components of Flock House virus cell entry. J. Virol. **83**: 8628–8637.
17. **Opie SR, Warrington KH, Jr, Agbandje-McKenna M, Zolotukhin S, Muzyczka N.** 2003. Identification of amino acid residues in the capsid proteins of adeno-associated virus type 2 that contribute to heparan sulfate proteoglycan binding. J. Virol. **77**:6995–7006.
18. **Sonntag F, Bleker S, Leuchs B, Fischer R, Kleinschmidt JA.** 2006. Adeno-associated virus type 2 capsids with externalized VP1/VP2 trafficking domains are generated prior to passage through the cytoplasm and are maintained until uncoating occurs in the nucleus. J. Virol. **80**:11040–11054.
19. **Thomas DL, et al.** 2009. Scalable recombinant adeno-associated virus production using recombinant herpes simplex virus type 1 coinfection of suspension-adapted mammalian cells. Hum. Gene Ther. **20**:861–870.
20. **Van Vliet K, Blouin V, Agbandje-McKenna M, Snyder RO.** 2006. Proteolytic mapping of the adeno-associated virus capsid. Mol. Ther. **14**: 809–821.
21. **Wobus CE, et al.** 2000. Monoclonal antibodies against the adeno-associated virus type 2 (AAV-2) capsid: epitope mapping and identification of capsid domains involved in AAV-2-cell interaction and neutralization of AAV-2 infection. J. Virol. **74**:9281–9293.
22. **Wu P, et al.** 2000. Mutational analysis of the adeno-associated virus type 2 (AAV2) capsid gene and construction of AAV2 vectors with altered tropism. J. Virol. **74**:8635–8647.
23. **Zolotukhin S, et al.** 2002. Production and purification of serotype 1, 2, and 5 recombinant adeno-associated viral vectors. Methods **28**:158–167.